Tetrahedron xxx (xxxx) xxx

Contents lists available at ScienceDirect

Tetrahedron

journal homepage: www.elsevier.com/locate/tet

Photoinduced copper-catalyzed dual decarboxylative coupling of α,β-unsaturated carboxylic acids with redox-active esters

Xiao-Yu Lu [a, b, *], Ang Gao [a], Qi-Le Liu [a], Ze-Jie Xia [a]

[a] College of Materials and Chemical Engineering, Chuzhou University, Hui Feng Road 1, Chuzhou, 239000, PR China
[b] School of Chemistry and Chemical Engineering, AnHui University, Hefei, 230601, China

ARTICLE INFO

Article history:
Received 23 March 2021
Received in revised form
6 May 2021
Accepted 24 May 2021
Available online xxx

Keywords:
Photoinduced
Copper-catalyzed
Decarboxylative
Unsaturated carboxylic acids
Redox-active esters

ABSTRACT

The first photoinduced copper-catalyzed dual decarboxylative cross-coupling of α,β-unsaturated carboxylic acids and redox-active esters has been developed. This reaction enabled C(sp^2)–C(sp^3) bond formation, which afforded a variety of synthetically valuable alkene derivatives. Many α,β-unsaturated carboxylic acids and redox-active ester derivatives were tolerant to this reaction. The reaction also tolerated many common functional groups.

1. Introduction

In the past few decades, transition metal-catalyzed cross-coupling reactions have become powerful methods for constructing carbon–carbon bonds. They have shown wide applicability for the synthesis of pharmaceutically-active compounds, agricultural chemicals, natural products, and functional materials [1–4]. Cinnamic acids are abundant compounds with broad structural diversity, natural and synthetic sources, and are common in many drug molecules and active natural products [5–8]. Recently, synthetic chemists have used inexpensive, stable, readily-available, and environmentally-friendly cinnamic acids (as per extraction by carbon dioxide) to construct C–C bonds, and various decarboxylative cross-couplings of cinnamic acids have been realized [9–13]; however, reported reactions require the use of transition metals and high temperatures to overcome unfavorable thermodynamics [14–17]. Therefore, the development of mild and eco-friendly decarboxylative coupling reactions of cinnamic acids is highly desired.

Recently, researchers have used mild photoinduced radical decarboxylative functionalization to create several nontraditional bond formation methods [18–20]. The photoredox catalytic decarboxylative cross-coupling of cinnamic acids has attracted considerable attention, but most of these reactions use costly and scarce iridium- or ruthenium-based photoredox catalysts because of their excellent photochemical properties [21–27]. As an alternative, copper salts are earth-abundant, inexpensive, and have low toxicities [28,29]. The development of copper as a photocatalyst under visible-light irradiation is still in its infancy [30–38]; thus, the photoinduced copper-catalyzed decarboxylative cross-coupling of cinnamic acids has rarely been reported (Scheme 1a) [39] (see Scheme 2).

Herein, we report the first example of the photoinduced copper-catalyzed dual decarboxylative cross-coupling of α,β-unsaturated carboxylic acids with redox-active esters (Scheme 1b). The reaction was tolerant to many synthetically valuable functional groups. Suitable substrates included primary, secondary, and tertiary carboxylic acids derived redox esters. The *E* isomer was preferred because of the thermodynamic stability of the product. Our photocatalytic dual decarboxylative cross-coupling method provides a route for the modification of complex organic molecules containing carboxylic acids and requires neither rare metals nor preformed metal photocatalyst.

* Corresponding author. College of Materials and Chemical Engineering, Chuzhou University, Hui Feng Road 1, Chuzhou, 239000, PR China.
E-mail address: xiaoyulu@mail.ustc.edu.cn (X.-Y. Lu).

https://doi.org/10.1016/j.tet.2021.132259
0040-4020/

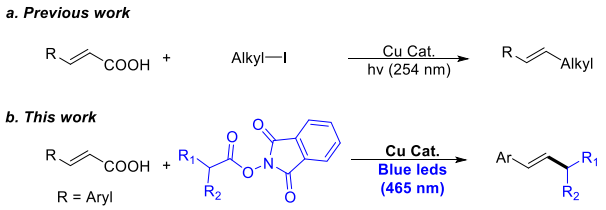

Scheme 1. Photoinduced copper-catalyzed decarboxylative coupling of α,β-unsaturated carboxylic acids.

2. Results and discussion

We first selected cinnamic acid (**1a**) and a cyclohexyl carboxylic acid derived redox-active NHPI ester (**2a**) as model reactants. Based on previous research, we first used $Cu(MeCN)_4PF_6$ as catalyst, L1 and Xantphos as ligands, and DMAc as solvent under irradiation by 20 W blue LEDs at room temperature. We obtained the product in 49% yield (entry 1). We then screened a series of solvents, including DMF, CH_3CN, THF, DMSO, and CH_2Cl_2 (entry 2–6), but only THF provided a better yield than DMAc (entry 4). We then evaluated a range of nitrogen ligands, also in THF solvent (entry 7–10). Unfortunately, only the L4 ligand provided 15% yield (entry 7), and almost no product was obtained using other nitrogen ligands (entry 8–10). Finally, we obtained the optimal reaction conditions by adjusting the ratio of the amounts of reactants (entry 11–14). A control experiment indicated that no reaction occurred in the absence of $Cu(MeCN)_4PF_6$ or blue LEDs (entry 15 and 16).

With the optimized conditions in hand, we next investigated the substrate scope of the photoinduced copper-catalyzed dual decarboxylative reaction (Table 2). Many substituted α,β-unsaturated carboxylic acids, coupled with a series of aliphatic carboxylic acid derived redox-active esters, provided good yields and preferential *E* selectivity. Both electron-rich (such as methoxy, phenyl) and electron-poor (such as trifluoromethyl) cinnamic acids afforded products in excellent yields. This reaction was tolerant to many synthetically useful functional groups, including fluorine (**3d**), esters (**3f**), tetrahydropyran (**3i**, **3j**), amides (**3k**), and alkenes (**3l**). Beyond the styrene system, heterocycles such as furan (**3m**), thiophene (**3n**), and pyridine (**3o**), were also compatible, providing the corresponding products in good yields. Unprotected phenolic hydroxyl (**3h**) and aryl carboxylic acids (**3g**) were also compatible with our method. Acyclic primary carboxylic acid derived redox-active esters (**3n**, **3p**) also participated in the coupling reaction. Quaternary carboxylic acid derived redox-active esters were also suitable, giving the substituted quaternary alkene derivatives in high *E*-product stereoselectivity. We also tested some quaternary carboxylic acid derived redox-active ester substrates, and they all provided high yields (**3q**, **3r**, **3s**, **3t**, **3u**). To further demonstrate the compatibility of the copper-catalyzed dual decarboxylative cross-coupling, we examined several α,β-unsaturated carboxylic acids containing other coupling units. Aryl chloride (**3v**) and aryl bromide (**3w**) were well-tolerated, as was aryl tosylate (**3x**). These experiments demonstrate the broad compatibility and selectivity of the reaction and provide opportunities for convenient transformations at the retained coupling units by using other cross-coupling reactions.

Table 1
Optimization of the reaction conditions.

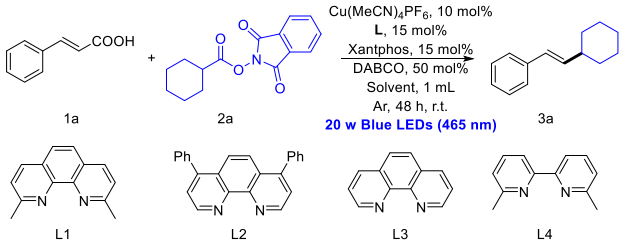

Entry	Ligand	Solvent	Yield%
1[a]	L1	DMA[c]	49
2[a]	L1	DMF	47
3[a]	L1	CH_3CN	42
4[a]	L1	THF	63
5[a]	L1	DMSO	51
6[a]	L1	CH_2Cl_2	32
7[a]	L4	THF	15
8[a]	L3	THF	trace
9[a]	L2	THF	trace
10[a]	dtbpy	THF	trace
11[b]	L1	THF	32
12[b]	L1	dio[e]ane	31
13[b]	L1	DMAc	26
14[c]	**L1**	**THF**	**78**
15[d]	L1	THF	0
16[e]	L1	THF	0

[a] Reaction conditions: 1a (0.2 mmol), 2a (0.4 mmol) in 1 mL solvent irradiated by 20 W blue LEDs for 48 h under Ar. 1a (0.4 mmol), 2a (0.2 mmol).
[b] 1a (0.4 mmol), 2a (0.2 mmol).
[c] 1a (0.2 mmol), 2a (0.6 mmol).
[d] No Cu Salt.
[e] No Blue LEDs. The yield was determined by GC using biphenyl as internal standard (see Table 1).

We next demonstrated the photoinduced copper-catalyzed dual decarboxylative cross-coupling reactions for the late-stage modification of natural products and drug molecules containing carboxylic acids. Treatment of a gemfibrozil derivative afforded product **4a** in 70% yield. Treating dehydrocholic acid derived redox-active esters containing three base-sensitive ketone groups afforded the desired product **4b** in 67% yield. Modification of a mycophenolic acid derived redox-active ester produced the corresponding product **4c** in moderate yield and tolerated the hydroxyl group. These results extensively demonstrate the broad applicability of this reaction for modifying complex natural products and drug molecules.

To gain insight into the reaction mechanism, we conducted control experiments. First, when we added 1 eq. of TEMPO (a common radical scavenger) to the model reaction, we obtained no desired product (Scheme 3, Eq. 1). Critically, treating (Z)-cinnamic acid with redox-active esters also afforded the *trans*-alkene product, which indicates that the stereoconvergent reaction proceeded by a radical process (Scheme 3, Eq. 2). Based on the above results and previous reports [30,40–43], a possible reaction mechanism was proposed, as depicted in Scheme 3. Initially, Cu^{+1} was excited to a reducing excited state $(Cu^{+1})^*$ by visible light irradiation. Next, a single-electron transfer from $(Cu^{+1})^*$ to NHP esters generated Cu^{+2} and a radical anion **I**, which then fragmented, followed by CO_2 evolution to produce an alkyl radical ($R^{\bullet}$). Radical addition of alkyl radical $R^{\bullet}$ to cinnamic acid provided the β-radical carboxylate **II** intermediate. The photoexcited Cu^{+2} then oxidized DABCO to give $DABCO^{+\bullet}$. Then, $DABCO^{+\bullet}$ was oxidized, accepting an electron from β-radical carboxylate **II** to complete the redox cycle. Finally, decarboxylation of **III** generated the product.

3. Conclusion

Here, we disclose the first photoinduced copper-catalyzed dual decarboxylative cross-coupling of α,β-unsaturated carboxylic acids with aliphatic carboxylic acid derived redox-active esters. This reaction enabled $C(sp^2)$–$C(sp^3)$ bond formation to access a variety of

Table 2
Scope of the dual decarboxylative coupling[a].

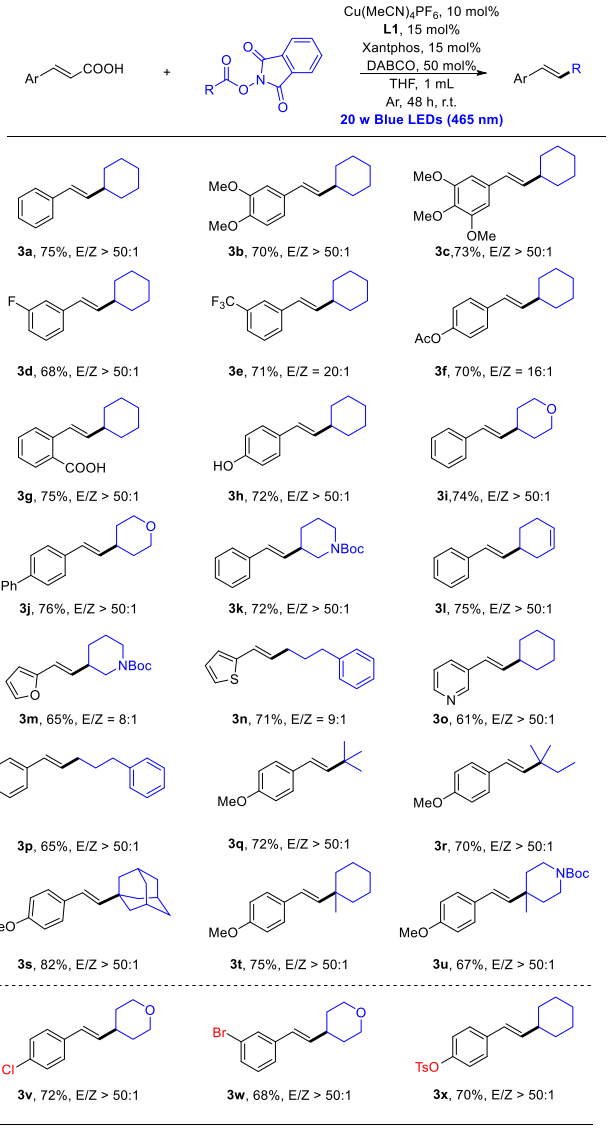

[a] Reaction conditions: $Cu(MeCN)_4PF_6$ (10 mol%), L1 (15 mol%), xantphos (15 mol%), DABCO (50 mol%), acrylic acids (0.2 mmol) and redox active ester (0.6 mmol). E/Z ratio was determined by ^1H NMR analysis.

[a] Reaction conditions: $Cu(MeCN)_4PF_6$ (10 mol%), L1 (15 mol%), xantphos (15 mol%), DABCO (50 mol%), acrylic acids (0.2 mmol) and redox active ester (0.6 mmol). E/Z ratio was determined by ^1H NMR analysis.

synthetically valuable alkene derivatives. A series of α,β-unsaturated carboxylic acids and redox-active esters derivatives was tolerant. The reaction was tolerant to many critical functional groups. Primary, secondary, and tertiary carboxylic acids derived redox-active esters were all suitable substrates. The *E* isomer was preferred due to the thermodynamic stability of the product. This also provides a route for modifying complex natural products and drug molecules containing carboxylic acids.

4. Experimental section

4.1. General procedure

In air, $Cu(MeCN)_4PF_6$ (10 mol%), L1 (15 mol%), xantphos (15 mol%), DABCO (50 mol%), α,β-unsaturated carboxylic acids (0.2 mmol) and redox active ester (0.6 mmol) were added to a schlenk tube equipped with a stir bar. The vessel was evacuated and filled with argon (three cycles). Anhydrous THF (1 mL) were added by syringe. The resulting reaction mixture was stirred under the irradiation of a 20 W blue LEDs (465 nm) at room temperature for 48 h under Ar. The resulting solution was purified by column chromatography.

4.2. (E)-(2-cyclohexylvinyl)benzene (**3a**)

White liquid. ^1H NMR (400 MHz, Chloroform-*d*) δ 7.35 (d, $J = 7.4$ Hz, 2H), 7.29 (t, $J = 7.6$ Hz, 2H), 7.18 (t, $J = 7.2$ Hz, 1H), 6.35 (d, $J = 16.0$ Hz, 1H), 6.18 (dd, $J = 16.0$, 6.9 Hz, 1H), 2.18–2.09 (m, 1H), 1.85–1.73 (m, 4H), 1.72–1.64 (m, 1H), 1.37–1.14 (m, 5H). ^{13}C NMR

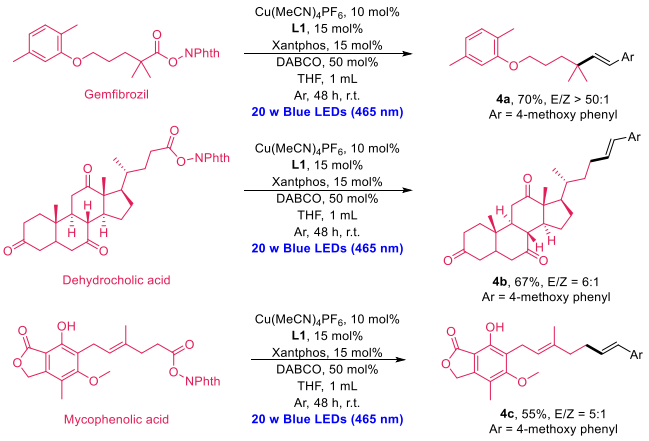

Scheme 2. Modification of natural products and drug molecules.

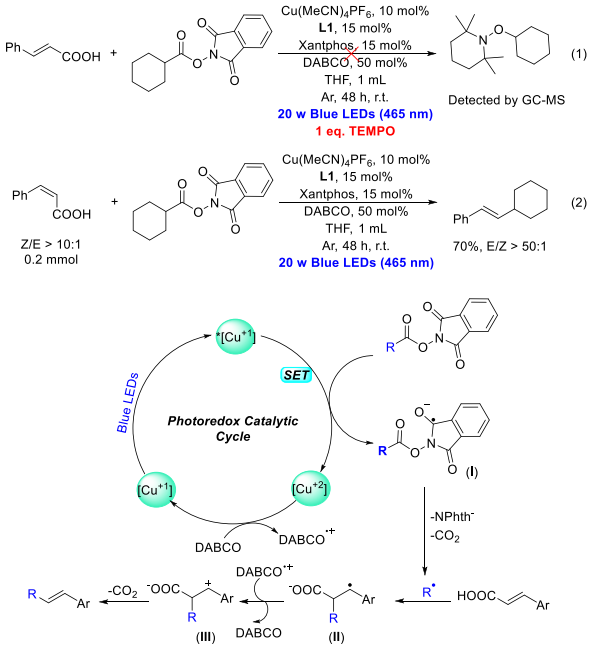

Scheme 3. Mechanism experiments and proposed catalytic cycle.

(101 MHz, Chloroform-*d*) δ 138.02, 136.84, 128.43, 127.16, 126.70, 125.90, 41.14, 32.93, 26.15, 26.03. HRMS (ESI) calcd for $C_{14}H_{19}$ ($M + H^+$): 187.1481; found: 187.1486.

4.3. (*E*)-4-(2-cyclohexylvinyl)-1,2-dimethoxybenzene (**3b**)

White solid. ^{1}H NMR (400 MHz, Chloroform-*d*) δ 6.91 (d, *J* = 1.8 Hz, 1H), 6.87 (dd, *J* = 8.2, 1.8 Hz, 1H), 6.79 (d, *J* = 8.2 Hz, 1H), 6.28 (d, *J* = 15.9 Hz, 1H), 6.04 (dd, *J* = 15.9, 7.0 Hz, 1H), 3.90 (s, 3H), 3.86 (s, 3H), 2.16–2.05 (m, 1H), 1.85–1.72 (m, 4H), 1.68 (d, *J* = 12.6 Hz, 1H), 1.35–1.25 (m, 2H), 1.24–1.13 (m, 3H). ^{13}C NMR (101 MHz, Chloroform-*d*) δ 148.88, 148.07, 134.94, 131.11, 126.76, 118.77, 111.05, 108.32, 55.84, 55.70, 41.06, 33.02, 26.12, 26.02. HRMS (ESI) calcd for $C_{16}H_{23}O_2$ ($M + H^+$): 247.1693; found: 247.1692.

4.4. (*E*)-5-(2-cyclohexylvinyl)-1,2,3-trimethoxybenzene (**3c**)

Pale-yellow liquid. ^{1}H NMR (400 MHz, Chloroform-*d*) δ 6.57 (s, 2H), 6.27 (d, *J* = 15.9 Hz, 1H), 6.08 (dd, *J* = 15.9, 6.9 Hz, 1H), 3.87 (s, 6H), 3.83 (s, 3H), 2.16–2.05 (m, 1H), 1.86–1.66 (m, 5H), 1.37–1.12 (m, 5H). ^{13}C NMR (101 MHz, Chloroform-*d*) δ 153.22, 137.09, 136.40, 133.80, 127.09, 102.84, 60.89, 56.00, 41.08, 32.95, 26.12, 26.01. HRMS (ESI) calcd for $C_{17}H_{25}O_3$ ($M + H^+$): 277.1798; found: 277.1796.

4.5. (*E*)-1-(2-cyclohexylvinyl)-3-fluorobenzene (**3d**)

White liquid. ^{1}H NMR (400 MHz, Chloroform-*d*) δ 7.24–7.20 (m, 1H), 7.11–7.01 (m, 2H), 6.90–6.82 (m, 1H), 6.30 (d, *J* = 16.0 Hz, 1H), 6.18 (dd, *J* = 16.0, 6.8 Hz, 1H), 2.12 (dtt, *J* = 13.7, 6.7, 3.3 Hz, 1H), 1.85–1.73 (m, 4H), 1.71–1.65 (m, 1H), 1.35–1.13 (m, 5H). ^{19}F NMR (376 MHz, Chloroform-*d*) δ −113.98. ^{13}C NMR (101 MHz, Chloroform-*d*) δ 163.11 (d, *J* = 244.7 Hz), 140.46 (d, *J* = 7.7 Hz), 138.23, 129.79 (d, *J* = 8.5 Hz), 126.24 (d, *J* = 2.5 Hz), 121.81 (d, *J* = 2.6 Hz), 113.44 (d, *J* = 21.4 Hz), 112.29 (d, *J* = 21.6 Hz), 41.08, 32.79, 26.10, 25.97. HRMS (ESI) calcd for $C_{14}H_{18}F$ ($M + H^+$): 205.1387; found: 205.1390.

4.6. (*E*)-1-(2-cyclohexylvinyl)-3-(trifluoromethyl)benzene (**3e**)

Pale-yellow liquid. ^{1}H NMR (400 MHz, Chloroform-*d*) δ 7.59–7.54 (m, 1H), 7.46–7.36 (m, 2H), 7.24–7.19 (m, 1H), 6.65 (d, *J* = 16.0 Hz, 1H), 6.53 (dd, *J* = 16.0, 6.8 Hz, 1H), 2.52–2.43 (m, 1H), 2.18–2.08 (m, 4H), 2.06–1.99 (m, 1H), 1.69–1.49 (m, 5H). ^{19}F NMR (376 MHz, Chloroform-*d*) δ −113.98. ^{13}C NMR (101 MHz, Chloroform-*d*) δ 138.85, 129.80 (q, *J* = 237.7 Hz), 129.16, 129.15, 128.86, 126.06, 125.59 (q, *J* = 3.2 Hz), 123.26 (q, *J* = 3.8 Hz), 122.56 (q, *J* = 3.8 Hz), 41.15, 32.77, 26.09, 25.96. HRMS (ESI) calcd for $C_{15}H_{18}F_3$ ($M + H^+$): 255.1355; found: 255.1357.

4.7. (*E*)-4-(2-cyclohexylvinyl)phenyl acetate (**3f**)

Pale-yellow liquid. ^{1}H NMR (400 MHz, Chloroform-*d*) δ 7.42–7.30 (m, 2H), 7.08–6.93 (m, 2H), 6.32 (d, *J* = 16.0 Hz, 1H), 6.12 (dd, *J* = 16.0, 6.9 Hz, 1H), 2.29 (s, 3H), 2.12 (dt, *J* = 7.5, 3.9 Hz, 1H), 1.87–1.64 (m, 5H), 1.39–1.06 (m, 5H). ^{13}C NMR (101 MHz, Chloroform-*d*) δ 169.73, 149.52, 137.30, 136.06, 126.95, 126.39, 121.65, 41.27, 33.05, 26.29, 26.16, 21.29. HRMS (ESI) calcd for $C_{16}H_{21}O_2$ ($M + H^+$): 245.1536; found: 245.1539.

4.8. (*E*)-2-(2-cyclohexylvinyl)benzoic acid (**3g**)

Pale-yellow liquid. ^{1}H NMR (400 MHz, Chloroform-*d*) δ 8.00 (dd, *J* = 7.9, 1.1 Hz, 1H), 7.58 (d, *J* = 7.9 Hz, 1H), 7.49 (td, *J* = 7.7, 1.2 Hz, 1H), 7.32–7.27 (m, 1H), 7.23 (d, *J* = 15.9 Hz, 1H), 6.11 (dd, *J* = 15.9, 6.9 Hz, 1H), 2.26–2.17 (m, 1H), 1.89–1.67 (m, 5H), 1.38–1.18 (m, 5H). ^{13}C NMR (101 MHz, Chloroform-*d*) δ 172.88, 140.96, 140.21, 132.95, 131.37, 127.54, 127.01, 126.65, 126.30, 41.40, 32.96, 26.31, 26.14. HRMS (ESI) calcd for $C_{15}H_{19}O_2$ ($M + H^+$): 231.1380; found: 231.1385.

4.9. (*E*)-4-(2-cyclohexylvinyl)phenol (**3h**)

Pale-yellow liquid. ^{1}H NMR (400 MHz, Chloroform-*d*) δ 7.23 (d, *J* = 8.6 Hz, 2H), 6.77 (d, *J* = 8.6 Hz, 2H), 6.28 (d, *J* = 16.0 Hz, 1H), 6.03 (dd, *J* = 16.0, 7.0 Hz, 1H), 5.08 (s, 1H), 2.17–1.99 (m, 1H), 1.88–1.72 (m, 4H), 1.73–1.61 (m, 1H), 1.39–1.09 (m, 5H). ^{13}C NMR (101 MHz, Chloroform-*d*) δ 154.37, 134.81, 131.02, 127.16, 126.41, 115.33, 41.06, 33.03, 26.14, 26.04. HRMS (ESI) calcd for $C_{14}H_{19}O$ ($M + H^+$): 203.1430; found: 203.1436.

4.10. (*E*)-4-styryltetrahydro-2H-pyran (**3i**)

Pale-yellow liquid. ^{1}H NMR (400 MHz, Chloroform-*d*) δ 7.36 (dd, *J* = 8.3, 1.2 Hz, 2H), 7.30 (td, *J* = 6.9, 6.5, 1.8 Hz, 2H), 7.24–7.18 (m, 1H), 6.39 (d, *J* = 16.0 Hz, 1H), 6.16 (dd, *J* = 16.0, 6.8 Hz, 1H),

4.05–3.97 (m, 2H), 3.47 (td, J = 11.7, 2.3 Hz, 2H), 2.44–2.34 (m, 1H), 1.75–1.66 (m, 2H), 1.63–1.54 (m, 2H). ^{13}C NMR (101 MHz, Chloroform-*d*) δ 137.64, 134.72, 128.66, 128.37, 127.22, 126.15, 67.86, 38.50, 32.74. HRMS (ESI) calcd for $C_{13}H_{17}O$ (M + H^+): 189.1274; found: 189.1277.

4.11. (E)-4-(2-([1,1′-biphenyl]-4-yl)vinyl)tetrahydro-2H-pyran (**3j**)

Pale-yellow solid. ^{1}H NMR (400 MHz, Chloroform-*d*) δ 7.64–7.54 (m, 4H), 7.48–7.42 (m, 4H), 7.39–7.31 (m, 1H), 6.44 (d, J = 15.9 Hz, 1H), 6.22 (dd, J = 16.0, 6.8 Hz, 1H), 4.08–3.99 (m, 2H), 3.49 (td, J = 11.7, 2.2 Hz, 2H), 2.47–2.37 (m, 1H), 1.78–1.70 (m, 2H), 1.66–1.55 (m, 2H). ^{13}C NMR (101 MHz, Chloroform-*d*) δ 140.71, 139.79, 136.53, 134.72, 128.72, 127.76, 127.17, 126.84, 126.40, 67.69, 38.39, 32.58. HRMS (ESI) calcd for $C_{19}H_{21}O$ (M + H^+): 265.1587; found: 265.1589.

4.12. Tert-butyl (E)-3-styrylpiperidine-1-carboxylate (**3k**)

Pale-yellow solid. ^{1}H NMR (400 MHz, Chloroform-*d*) δ 7.37–7.28 (m, 4H), 7.22 (d, J = 7.1 Hz, 1H), 6.45 (d, J = 16.0 Hz, 1H), 6.09 (dd, J = 16.1, 7.0 Hz, 1H), 3.98 (d, J = 13.2 Hz, 2H), 2.83–2.74 (m, 1H), 2.68 (s, 1H), 2.37–2.27 (m, 1H), 1.96–1.90 (m, 1H), 1.71 (dt, J = 13.1, 3.6 Hz, 1H), 1.57–1.51 (m, 1H), 1.47 (s, 9H), 1.42–1.32 (m, 1H). ^{13}C NMR (101 MHz, Chloroform-*d*) δ 154.99, 137.49, 131.92, 129.90, 128.65, 127.32, 126.16, 79.53, 49.21, 44.30, 39.49, 31.01, 28.60, 24.86. HRMS (ESI) calcd for $C_{18}H_{26}NO_2$ (M + H^+): 288.1958; found: 288.1963.

4.13. (E)-(2-(cyclohex-3-en-1-yl)vinyl)benzene (**3l**)

Pale-yellow liquid. ^{1}H NMR (400 MHz, Chloroform-*d*) δ 7.38 (d, J = 7.4 Hz, 2H), 7.32 (t, J = 7.6 Hz, 2H), 7.21 (t, J = 7.3 Hz, 1H), 6.43 (d, J = 16.0 Hz, 1H), 6.26 (dd, J = 15.9, 7.2 Hz, 1H), 5.74 (d, J = 1.9 Hz, 2H), 2.50–2.42 (m, 1H), 2.28–2.19 (m, 1H), 2.15 (dt, J = 6.2, 3.7 Hz, 2H), 2.04–1.94 (m, 1H), 1.91–1.83 (m, 1H), 1.56–1.49 (m, 1H). ^{13}C NMR (101 MHz, Chloroform-*d*) δ 137.96, 135.85, 128.61, 128.09, 127.12, 126.99, 126.16, 126.12, 37.25, 31.52, 28.87, 24.97. HRMS (ESI) calcd for $C_{14}H_{17}$ (M + H^+): 185.1325; found: 185.1328.

4.14. Tert-butyl (E)-3-(2-(furan-2-yl)vinyl)piperidine-1-carboxylate (**3m**)

Pale-yellow liquid. ^{1}H NMR (400 MHz, Chloroform-*d*) δ 7.34–7.29 (m, 1H), 6.34 (dd, J = 3.2, 1.9 Hz, 1H), 6.25 (d, J = 16.2 Hz, 1H), 6.16 (d, J = 3.1 Hz, 1H), 6.03 (dd, J = 16.1, 7.0 Hz, 1H), 3.95 (d, J = 12.7 Hz, 2H), 2.80–2.72 (m, 1H), 2.67 (s, 1H), 2.27 (dt, J = 6.8, 3.5 Hz, 1H), 1.90 (dd, J = 9.2, 3.7 Hz, 1H), 1.75–1.66 (m, 2H), 1.46 (s, 9H), 1.32 (dd, J = 19.0, 7.2 Hz, 1H). ^{13}C NMR (101 MHz, Chloroform-*d*) δ 154.97, 152.99, 141.65, 130.72, 118.53, 111.32, 107.05, 79.56, 49.17, 44.12, 39.22, 30.88, 28.59, 24.68. HRMS (ESI) calcd for $C_{16}H_{24}NO_3$ (M + H^+): 278.1751; found: 278.1752.

4.15. (E)-2-(5-phenylpent-1-en-1-yl)thiophene (**3n**)

Pale-yellow liquid. ^{1}H NMR (400 MHz, Chloroform-*d*) δ 7.34–7.31 (m, 2H), 7.22 (dt, J = 7.7, 1.0 Hz, 3H), 7.11 (dt, J = 5.0, 0.9 Hz, 1H), 6.96 (dd, J = 5.1, 3.5 Hz, 1H), 6.90–6.88 (m, 1H), 6.58–6.51 (m, 1H), 6.15–6.05 (m, 1H), 2.71–2.66 (m, 2H), 2.28–2.21 (m, 2H), 1.87–1.78 (m, 2H). ^{13}C NMR (101 MHz, Chloroform-*d*) δ 143.16, 142.38, 130.66, 128.59, 128.44, 127.34, 125.88, 124.39, 123.60, 123.26, 35.47, 32.44, 30.99. HRMS (ESI) calcd for $C_{15}H_{17}S$ (M + H^+): 229.1045; found: 229.1048.

4.16. (E)-3-(2-cyclohexylvinyl)pyridine (**3o**)

Pale-yellow liquid. ^{1}H NMR (400 MHz, Chloroform-*d*) δ 8.55 (s, 1H), 8.41 (d, J = 4.2 Hz, 1H), 7.68 (d, J = 7.9 Hz, 1H), 7.23 (dd, J = 7.8, 4.9 Hz, 1H), 6.43–6.15 (m, 2H), 2.15 (t, J = 14.4, 6.5, 3.3 Hz, 1H), 1.85–1.74 (m, 4H), 1.69 (d, J = 12.7 Hz, 1H), 1.38–1.10 (m, 5H). ^{13}C NMR (101 MHz, Chloroform-*d*) δ 147.71, 147.49, 139.69, 133.94, 132.93, 123.71, 123.63, 41.39, 32.84, 26.21, 26.08. HRMS (ESI) calcd for $C_{13}H_{18}N$ (M + H^+): 188.1434; found: 188.1436.

4.17. (E)-pent-1-ene-1,5-diyldibenzene (**3p**)

Pale-yellow liquid. ^{1}H NMR (400 MHz, Chloroform-*d*) δ 7.36 (dd, J = 8.2, 1.2 Hz, 2H), 7.33–7.27 (m, 4H), 7.23–7.18 (m, 4H), 6.41 (d, J = 15.8 Hz, 1H), 6.25 (dt, J = 15.8, 6.8 Hz, 1H), 2.72–2.65 (m, 2H), 2.31–2.23 (m, 2H), 1.87–1.78 (m, 2H). ^{13}C NMR (101 MHz, Chloroform-*d*) δ 142.50, 137.93, 130.69, 130.34, 128.62, 128.44, 127.00, 126.06, 125.86, 35.53, 32.67, 31.16. HRMS (ESI) calcd for $C_{17}H_{19}$ (M + H^+): 223.1481; found: 223.1480.

4.18. (E)-1-(3,3-dimethylbut-1-en-1-yl)-4-methoxybenzene (**3q**)

Pale-yellow liquid. ^{1}H NMR (400 MHz, Chloroform-*d*) δ 7.33–7.28 (m, 2H), 6.88–6.81 (m, 2H), 6.26 (d, J = 16.2 Hz, 1H), 6.13 (d, J = 16.2 Hz, 1H), 3.81 (s, 3H), 1.12 (s, 9H). ^{13}C NMR (101 MHz, Chloroform-*d*) δ 158.71, 139.95, 130.96, 127.18, 123.97, 114.03, 55.42, 33.38, 29.83. HRMS (ESI) calcd for $C_{13}H_{19}O$ (M + H^+): 191.1430; found: 191.1432.

4.19. (E)-1-(3,3-dimethylpent-1-en-1-yl)-4-methoxybenzene (**3r**)

Pale-yellow liquid. ^{1}H NMR (400 MHz, Chloroform-*d*) δ 7.33 (d, J = 8.7 Hz, 2H), 6.87 (d, J = 8.8 Hz, 2H), 6.26 (d, J = 16.2 Hz, 1H), 6.06 (d, J = 16.2 Hz, 1H), 3.82 (s, 3H), 1.44 (q, J = 7.5 Hz, 2H), 1.10 (s, 6H), 0.87 (t, J = 7.5 Hz, 3H). ^{13}C NMR (101 MHz, Chloroform-d) δ 158.70, 138.64, 131.06, 127.14, 125.28, 114.00, 55.38, 36.39, 35.70, 26.93, 9.17. HRMS (ESI) calcd for $C_{14}H_{21}O$ (M + H^+): 205.1587; found: 205.1586.

4.20. (3r,5r,7r)-1-((E)-4-methoxystyryl)adamantane (**3s**)

Pale-yellow liquid. ^{1}H NMR (400 MHz, Chloroform-*d*) δ 7.30 (d, J = 8.7 Hz, 2H), 6.85 (d, J = 8.7 Hz, 2H), 6.20 (d, J = 16.2 Hz, 1H), 5.98 (d, J = 16.2 Hz, 1H), 3.81 (s, 3H), 2.03 (s, 3H), 1.82–1.64 (m, 12H). ^{13}C NMR (101 MHz, Chloroform-d) δ 158.69, 140.25, 131.11, 127.14, 123.90, 114.01, 55.42, 42.47, 37.04, 35.16, 28.64. HRMS (ESI) calcd for $C_{19}H_{25}O$ (M + H^+): 269.1900; found: 269.1903.

4.21. (E)-1-methoxy-4-(2-(1-methylcyclohexyl)vinyl)benzene (**3t**)

Pale-yellow solid. ^{1}H NMR (400 MHz, Chloroform-*d*) δ 7.34–7.28 (m, 2H), 6.91–6.80 (m, 2H), 6.28 (d, J = 16.4 Hz, 1H), 6.09 (d, J = 16.4 Hz, 1H), 3.81 (s, 3H), 1.65–1.57 (m, 2H), 1.56–1.49 (m, 4H), 1.46–1.34 (m, 4H), 1.08 (s, 3H). ^{13}C NMR (101 MHz, Chloroform-d) δ 158.69, 139.10, 131.19, 127.07, 125.35, 114.01, 55.41, 38.18, 36.16, 27.77, 26.48, 22.59. HRMS (ESI) calcd for $C_{16}H_{23}O$ (M + H^+): 231.1743; found: 231.1748.

4.22. Tert-butyl (E)-4-(4-methoxystyryl)-4-methylpiperidine-1-carboxylate (**3u**)

Pale-yellow liquid. ^{1}H NMR (400 MHz, Chloroform-*d*) δ 7.34–7.22 (m, 2H), 6.85 (d, J = 8.7 Hz, 2H), 6.29 (d, J = 16.4 Hz, 1H), 6.02 (d, J = 16.4 Hz, 1H), 3.80 (s, 3H), 3.58–3.44 (m, 2H), 3.40–3.30 (m, 2H), 1.70–1.62 (m, 2H), 1.49–1.39 (m, 11H), 1.12 (s, 3H). ^{13}C NMR

(101 MHz, Chloroform-d) δ 158.96, 155.09, 136.50, 130.47, 127.18, 126.74, 114.06, 79.36, 55.41, 40.68, 37.09, 34.78, 28.58, 27.05. HRMS (ESI) calcd for $C_{20}H_{30}NO_3$ ($M + H^+$): 332.2220; found: 332.2225.

*4.23. (E)-4-(4-chlorostyryl)tetrahydro-2H-pyran (**3v**)*

Pale-yellow solid. ^{1}H NMR (400 MHz, Chloroform-*d*) δ 7.31–7.20 (m, 4H), 6.33 (dd, J = 16.0, 1.2 Hz, 1H), 6.13 (dd, J = 16.0, 6.8 Hz, 1H), 4.03–3.95 (m, 2H), 3.46 (td, J = 11.7, 2.3 Hz, 2H), 2.42–2.29 (m, 1H), 1.74–1.66 (m, 2H), 1.62–1.48 (m, 2H). ^{13}C NMR (101 MHz, Chloroform-d) δ 136.14, 135.39, 132.73, 128.76, 127.36, 127.22, 67.80, 38.47, 32.63. HRMS (ESI) calcd for $C_{13}H_{16}ClO$ ($M + H^+$): 223.0884; found: 223.0887.

*4.24. (E)-4-(3-bromostyryl)tetrahydro-2H-pyran (**3w**)*

Pale-yellow liquid. ^{1}H NMR (400 MHz, Chloroform-*d*) δ 7.50 (t, J = 1.8 Hz, 1H), 7.35–7.30 (m, 1H), 7.26–7.23 (m, 1H), 7.16 (t, J = 7.8 Hz, 1H), 6.31 (d, J = 16.1 Hz, 1H), 6.16 (dd, J = 16.0, 6.7 Hz, 1H), 4.05–3.97 (m, 2H), 3.46 (td, J = 11.7, 2.3 Hz, 2H), 2.38 (dtd, J = 10.6, 6.7, 2.9 Hz, 1H), 1.72–1.66 (m, 2H), 1.61–1.52 (m, 2H). ^{13}C NMR (101 MHz, Chloroform-d) δ 139.84, 136.31, 130.14, 130.04, 128.99, 127.08, 124.89, 122.86, 67.78, 38.47, 32.58. HRMS (ESI) calcd for $C_{13}H_{16}BrO$ ($M + H^+$): 267.0379; found: 267.0381.

*4.25. (E)-4-(2-cyclohexylvinyl)phenyl 4-methylbenzenesulfonate (**3x**)*

Pale-yellow liquid. ^{1}H NMR (400 MHz, Chloroform-*d*) δ 7.69 (d, J = 8.3 Hz, 2H), 7.30 (d, J = 8.1 Hz, 2H), 7.24–7.20 (m, 2H), 6.91–6.85 (m, 2H), 6.27 (d, J = 16.0 Hz, 1H), 6.11 (dd, J = 16.0, 6.9 Hz, 1H), 2.44 (s, 3H), 2.10 (ddp, J = 10.4, 6.8, 3.3 Hz, 1H), 1.79–1.64 (m, 5H), 1.35–1.09 (m, 5H). ^{13}C NMR (101 MHz, Chloroform-d) δ 148.37, 145.40, 138.12, 137.19, 132.49, 129.85, 128.69, 127.02, 126.04, 122.51, 41.26, 32.96, 26.22, 26.10, 21.85. HRMS (ESI) calcd for $C_{21}H_{25}O_3S$ ($M + H^+$): 357.1519; found: 357.1525.

*4.26. (E)-2-((6-(4-methoxyphenyl)-4,4-dimethylhex-5-en-1-yl) oxy)-1,4-dimethylbenzene (**4a**)*

Pale-yellow solid. ^{1}H NMR (400 MHz, Chloroform-*d*) δ 7.40–7.30 (m, 2H), 7.05 (d, J = 7.5 Hz, 1H), 6.94–6.83 (m, 2H), 6.76–6.63 (m, 2H), 6.31 (d, J = 16.2 Hz, 1H), 6.11 (d, J = 16.2 Hz, 1H), 3.96 (t, J = 6.4 Hz, 2H), 3.84 (s, 3H), 2.34 (s, 3H), 2.24 (s, 3H), 1.88–1.75 (m, 2H), 1.66–1.53 (m, 2H), 1.18 (s, 6H). ^{13}C NMR (101 MHz, Chloroform-*d*) δ 158.74, 157.14, 138.25, 136.50, 130.80, 130.33, 127.16, 125.49, 123.63, 120.64, 113.99, 112.02, 68.46, 55.35, 39.52, 36.05, 27.45, 25.06, 21.49, 15.92. HRMS (ESI) calcd for $C_{23}H_{31}O_2$ ($M + H^+$): 339.2319; found: 339.2325.

*4.27. (8R,9S,10S,13R,14S,17R)-17-((R,E)-6-(4-methoxyphenyl)hex-5-en-2-yl)-10,13-dimethyldodecahydro-3H-cyclopenta[a] phenanthrene-3,7,12(2H,4H)-trione (4**b**)*

Pale-yellow solid. ^{1}H NMR (400 MHz, Chloroform-*d*) δ 7.29–7.19 (m, 2H), 6.85 (ddd, J = 14.2, 8.6, 1.8 Hz, 2H), 6.32 (d, J = 16.1 Hz, 1H), 6.10–6.00 (m, 1H), 3.80 (s, 3H), 2.94–2.80 (m, 3H), 2.38–2.18 (m, 7H), 2.16–1.92 (m, 7H), 1.90–1.79 (m, 1H), 1.60 (q, J = 8.9, 6.4 Hz, 2H), 1.40 (s, 3H), 1.28 (dd, J = 10.4, 5.5 Hz, 4H), 1.07 (s, 3H), 0.91–0.81 (m, 3H). ^{13}C NMR (101 MHz, Chloroform-*d*) δ 212.17, 209.23, 208.92, 158.68, 130.82, 129.97, 129.22, 129.05, 127.05, 113.98, 57.01, 55.37, 51.87, 49.09, 46.93, 45.98, 45.63, 45.08, 42.89, 38.75, 36.58, 36.09, 35.77, 35.39, 35.35, 30.22, 27.93, 25.28, 21.99, 18.99, 11.97. HRMS (ESI) calcd for $C_{32}H_{43}O_4$ ($M + H^+$): 491.3156; found: 491.3159.

*4.28. 7-Hydroxy-5-methoxy-6-((2E,6E)-7-(4-methoxyphenyl)-3-methylhepta-2,6-dien-1-yl)-4-methylisobenzofuran-1(3H)-one (**4c**)*

Pale-yellow liquid. ^{1}H NMR (400 MHz, Chloroform-*d*) δ 7.67 (d, J = 2.0 Hz, 1H), 7.18 (dd, J = 8.5, 6.4 Hz, 2H), 6.78 (d, J = 8.7 Hz, 2H), 6.32–6.19 (m, 1H), 6.04–5.92 (m, 1H), 5.26–5.14 (m, 3H), 3.79 (s, 3H), 3.73 (s, 3H), 3.39 (d, J = 6.9 Hz, 2H), 2.44–2.23 (m, 2H), 2.13 (d, J = 12.2 Hz, 5H), 1.81 (s, 3H). ^{13}C NMR (101 MHz, Chloroform-*d*) δ 173.09, 163.70, 158.63, 153.73, 143.98, 135.28, 130.76, 129.99, 129.29, 128.45, 126.99, 122.51, 116.76, 113.88, 113.62, 106.42, 70.14, 61.09, 55.38, 39.60, 31.49, 22.73, 16.31, 11.65. HRMS (ESI) calcd for $C_{25}H_{29}O_5$ ($M + H^+$): 409.2010; found: 409.2013.

Declaration of competing interest

The authors declare that they have no known competing financial interests or personal relationships that could have appeared to influence the work reported in this paper.

Acknowledgement

We are grateful for the support from National Natural Science Foundation of China (22001029), Natural Science Foundation of Anhui Province (2008085QB92), and University Natural Science Research Key Project of Anhui Province (KJ2020A0708).

Appendix A. Supplementary data

Supplementary data to this article can be found online at https://doi.org/10.1016/j.tet.2021.132259.

References

[1] R. Jana, T.P. Pathak, M.S. Sigman, Chem. Rev. 111 (2011) 1417–1492.
[2] S.Z. Tasker, E.A. Standley, T.F. Jamison, Nature 509 (2014) 299–309.
[3] N. Kambe, T. Iwasaki, J. Terao, Chem. Soc. Rev. 40 (2011) 4937–4947.
[4] J.D. Weaver, A. Recio, A.J. Grenning, J.A. Tunge, Chem. Rev. 111 (2011) 1846–1913.
[5] M. Sova, Mini Rev. Med. Chem. 12 (2012) 749–767.
[6] K.C. Nicolaou, Q. Kang, S.Y. Ng, D.Y. Chen, J. Am. Chem. Soc. 132 (2010) 8219–8222.
[7] Q. Zhou, X. Chen, D. Ma, Angew. Chem. Int. Ed. 49 (2010) 3513–3516.
[8] D. Sun, Q. Zhao, C. Li, Org. Lett. 13 (2011) 5302–5305.
[9] L. Chen, L. Zhang, G. Yan, D. Huang, Asian J. Org. Chem. 9 (2020) 842–862.
[10] J. Ji, P. Liu, P. Sun, Chem. Commun. 51 (2015) 7546–7549.
[11] X. Zhu, M. Han, P. Li, L. Wang, Org. Chem. *Front*. 4 (2017) 1640–1646.
[12] Y. Yang, C. Xie, Y. Xie, Y. Zhang, Org. Lett. 14 (2012) 957–959.
[13] S. Yang, T. He, D. Lin, J. Huang, Org. Lett. 21 (2019) 1958–1962.
[14] A.J. Borah, G. Yan, Org. Biomol. Chem. 13 (2015) 8094–8115.
[15] J.-F. Zhao, X.-H. Duan, Y.-R. Gu, P. Gao, L.-N. Guo, Org. Lett. 20 (2018) 4614–4617.
[16] S. Han, X. Ren, Q. Wu, A. Liang, J. Li, D. Zou, Y. Wu, Y. Wu, Adv. Synth. Catal. 360 (2018) 2308–2312.
[17] X.-Y. Lu, J.-S. Li, S.-Q. Wang, Y.-J. Zhu, Y.-M. Li, L.-Y. Yan, J.-M. Li, J.-Y. Wang, H.-P. Zhou, X.-T. Ge, Chem. Commun. 55 (2019) 11123–11126.
[18] M.H. Shaw, J. Twilton, D.W.C. MacMillan, J. Org. Chem. 81 (2016) 6898–6926.
[19] M.N. Hopkinson, A. Tlahuext-Aca, F. Glorius, *Acc. Chem. Res.* 49 (2016) 2261–2272.
[20] J.J. Douglas, M.J. Sevrin, C.R.J. Stephenson, Org. Process Res. Dev. 20 (2016) 1134–1147.
[21] J. Twilton, C. Le, P. Zhang, M.H. Shaw, R.W. Evans, D.W.C. MacMillan, Nat. Rev. Chem. 1 (2017), 0052.
[22] J. Xuan, W.-J. Xiao, Angew. Chem. Int. Ed. 51 (2012) 6828–6838.
[23] N.A. Romero, D.A. Nicewicz, Chem. Rev. 116 (2016) 10075–10166.
[24] K. Xu, Z. Tan, H. Zhang, J. Liu, S. Zhang, Z. Wang, Chem. Commun. 53 (2017) 10719–10722.
[25] J.J. Zhang, J.C. Yang, L.N. Guo, X.H. Duan, Chem. Eur J. 23 (2017) 10259–10263.
[26] Y.-T. Wang, M.-C. Fu, B. Zhao, R. Shang, Y. Fu, Chem. Commun. 56 (2020) 2495–2498.
[27] H.-Y. Wang, L.-J. Zhong, G.-F. Lv, Y. Li, J.-H. Li, Org. Biomol. Chem. 18 (2020) 5589–5593.
[28] L.-J. Cheng, N.P. Mankad, Chem. Soc. Rev. 49 (2020) 8036–8064.
[29] El-Hage, F.; Pospech, J. Copper Catalysis in Organic Synthesis, 2020, DOI: https://doi.org/10.1002/9783527826445.ch14, pp. 309-328.
[30] X.-L. Lyu, S.-S. Huang, H.-J. Song, Y.-X. Liu, Q.-M. Wang, Org. Lett. 21 (2019)

5728–5732.
[31] M. Zhong, X. Pannecoucke, P. Jubault, T. Poisson, Beilstein J. Org. Chem. 16 (2020) 451–481.
[32] H. Chen, L.-X. Xu, L.-J. Yan, X.-F. Liu, D.-D. Xu, X.-C. Yu, J.-X. Fan, Q.-A. Wu, S.-P. Luo, Dyes Pigments 173 (2020) 108000.
[33] C. Wang, M. Guo, R. Qi, Q. Shang, Q. Liu, S. Wang, L. Zhao, R. Wang, Z. Xu, Angew. Chem. Int. Ed. 57 (2018) 15841–15846.
[34] Q. Guo, M. Wang, Q. Peng, Y. Huo, Q. Liu, R. Wang, Z. Xu, ACS Catal. 9 (2019) 4470–4476.
[35] T. Xu, T. Cao, M. Yang, R. Xu, X. Nie, S. Liao, Org. Lett. 22 (2020) 3692–3696.
[36] L. Zheng, Q. Jiang, H. Bao, B. Zhou, S.-P. Luo, H. Jin, H. Wu, Y. Liu, Org. Lett. 22 (2020) 8888–8893.
[37] D.-Y. Liu, X. Liu, Y. Gao, C.-Q. Wang, J.-S. Tian, T.-P. Loh, Org. Lett. 22 (2020) 8978–8983.
[38] T. öldesi, G. Sipos, R. Adamik, B. Nagy, B.L. Tóth, A. Bényei, K.J. Szekeres, G.G. Láng, A. Demeter, T.J. Peelen, Z. Novák, Org. Biomol. Chem. 17 (2019) 8343–8347.
[39] C. Wang, Y. Lei, M. Guo, Q. Shang, H. Liu, Z. Xu, R. Wang, Org. Lett. 19 (2017) 6412–6415.
[40] H. Liu, Q. Guo, C. Chen, M. Wang, Z. Xu, Org. Chem. Front. 5 (2018) 1522–1526.
[41] G. Li, T. Wang, F. Fei, Y.-M. Su, Y. Li, Q. Lan, X.-S. Wang, Angew. Chem. Int. Ed. 55 (2016) 3491.
[42] R. Kancherla, K. Muralirajan, B. Maity, C. Zhu, P.E. Krach, L. Cavallo, M. Rueping, Angew. Chem. Int. Ed. 58 (2019) 3412–3416.
[43] A. Baralle, L. Fensterbank, J.-P. Goddard, C. Ollivier, Chem. Eur J. 19 (2013) 10809–10813.